High-Throughput Synthesis and Characterisation of Eu Doped $Sr_xBa_{2-x}SiO_4$ Thin Film Phosphors

Sara Frost[1], Samuel Guérin[1], Brian E Hayden[1,2], Jean-Philippe Soulié[1] and Chris Vian[1]

1. Ilika Technologies, Dibben Kenneth House, Enterprise Road, University of Southampton Science Park, Chilworth, Southampton, SO16 7NS, UK.
2. Chemistry, University of Southampton, Highfield, Southampton, SO17 1BJ, UK.

Abstract

High-Throughput techniques have been employed for the synthesis and characterisation of thin film phosphors of Eu doped $Ba_xSr_{2-x}SiO_4$. Direct synthesis from evaporation of the constituent elements under a flux of atomic oxygen on a sapphire substrate at 850 °C was used to directly produce thin film libraries (415 nm thickness) of the crystalline orthosilicate phase with the desired compositional variation ($0.24 > x > 1.86$). The orthosilicate phase could be synthesised as a pure, or predominantly pure, phase. Annealing the as synthesised library in a reducing atmosphere resulted in the reduction of the Eu while retaining the orthosilicate phase, and resulted in a materials thin film library where fluorescence excited by blue light (450 nm) was observable by the naked eye. Parallel screening of the fluorescence from the combinatorial libraries of Eu doped $Ba_xSr_{2-x}SiO_4$ has been implemented by imaging the fluorescent radiation over the library using a monochrome digital camera using a series of colour filters. Informatics tools have been developed to allow the 1931 CIE

colour co-ordinates and the relative quantum efficiencies of the materials library to be rapidly assessed and mapped against composition and crystal structure and phase purity. The range of compositions gave values of CIE x between 0.17 and 0.52 and CIE y between 0.48 and 0.69 with relative efficiencies in the range 2.0 x 10^{-4} to 7.6 x 10^{-4}. Good agreement was obtained between the thin film phosphors and the fluorescence characteristics of a number of corresponding bulk phosphor powders. The thermal quenching of fluorescence in the thin film libraries was also measured in the temperature range 25-130°C: The phase purity of the thin film was found to significantly influence both the relative quantum efficiency and the thermal quenching of the fluorescence.

Keywords

phosphors, Eu, orthosilicate, combinatorial, high-throughput, thin film, PVD, fluorescence

Introduction

Research and development of phosphor compounds has been an active field of research for most of the 20th century with increases in research activity during the late 60s and 70s due to the advent of colour CRT displays.[1-3] In the 90s, interest in flat panel displays and X-rays imaging systems fuelled further research efforts.[4] More recently the emergence of solid-state white lighting using a combination of relatively high energy emission LEDs and down-converting phosphors has led to a renewed interest in the field.[5-10] The late 90s also saw the establishment of inorganic combinatorial material research as a new approach for material discovery, and some of the early work exemplifying the power of the high-throughput approach were in the search for new phosphors. Conventional synthetic methodologies based on aqueous[11-15] or powder[16-18] precursors were developed, although the largest combinatorial libraries of materials were synthesised using the physical vapour deposition (sputtering or laser ablation) of oxide precursors. [4, 19-21]: sequential deposition of precursors and subsequent annealing was used to produce the final materials. Photoluminescence (or in one case catholuminescence) [19] was characterised by sequential spectroscopic measurement of the emission spectrum, and this was often converted to the CIE system of colour co-ordinates.

We demonstrate here the advantages of simultaneous evaporative PVD[22] in the combinatorial synthesis of structurally characterised compositional gradient thin film libraries of Eu doped $Ba_xSr_{2-x}SiO_4$. When using a parallel fluorescent screening methodology combined with the appropriate informatics platform, we show an effective route to determining the compositional and structural dependence of the characteristic fluorescence: The colour co-ordinate, the relative quantum efficiency and the thermal quenching characteristics.

In the field of materials used for photoluminescence many crystal structures and active elements have been tried and reported.[23] Materials have been optimised sequentially to provide a specific emission wavelength in order to enable the production of white LEDs. Several approaches can be taken to achieve a white light LED: An important example is the combination of the emission of the blue light of a GaN LED with several down-converting phosphors in order to achieve the required white light.[5-10] In the simplest approach, yellow phosphors are used with blue LEDs to produce white light. “Warmer” white light LEDs are achieved by combining several phosphors, such as yellow/orange and red phosphors. Phosphors fluorescing in different parts of the visible spectrum are obtained by using different crystal families and active elements: Green can be obtained by using europium and barium orthosilicate,[24] yellow with cerium and a garnet structure[25] and red using europium and strontium nitridosilicate[10] or oxynitrides.[16, 18] Further tuning of the emission colour can be achieved by atomic substitutions of elements within the crystal structure.[7, 12, 26] One such crystal system which has been relatively extensively studied is the Eu doped alkaline orthosilicate,[1, 8, 24, 27-29], and alternative active elements from the rare earths have also been used.[30-35] Orthorhombic europium doped barium-strontium orthosilicates have been investigated extensively as a down conversion phosphor in both UV and blue LEDs system: They are characterised by high quantum yields, and the Ba to Sr ratio can be used to tune the florescent maxima in the range 511 to 574 nm.[26] Typically, this system is made by high temperature solid state reaction routes requiring firing at 1300 °C in a reducing atmosphere.[36]

Experimental

The compositionally graded thin films libraries created for the study of phosphors were deposited using a High-Throughput Physical Vapour Deposition (HTPVD) tool which enables the co-evaporation of the constituent elements. The combination of individual "wedge" shutters on each source combined with a plasma atom source for oxygen ensures that for every composition in the materials library the atomic species are being deposited simultaneously to facilitate a facile reaction to form the thermodynamically expected phase at relatively low substrate temperature.[22] The pure elements were loaded in either e-beam or Knudsen (effusion) evaporation sources. Ba (pieces 3-10 mm, 99.9% from Testbourne) was contained in a 40 cm^3 Ta crucible (DCA Instruments), Sr (pieces 3-6 mm, 99.9% pure from Testbourne) was contained in a 40 cm^3 alumina crucible (Almath Crucibles) and both were loaded in standard temperature effusion cells (DCA Instruments, T_{max} = 1400 °C). The Si (solid target, 99.999 % pure from Testbourne) was contained in a Ta crucible (Testbourne) to fit inside the 40 cm^3 copper body of a single pocket electron gun evaporation source (Telemark). The Eu (pieces 3-6 mm, 99.9% pure from Testbourne) was contained in a 25 cm^3 graphite crucible and loaded in a high temperature effusion cell (DCA Instruments, T_{max} = 2000 °C). The oxygen was provided via an in line RF discharge atom source (Oxford Applied Research) producing a beam of both neutral and charged atomic oxygen species. The evaporation system was pumped down and baked to achieve Ultra High Vacuum (UHV) with a base pressure of ca. $2x10^{-9}$ mbar. Evaporation rates and wedge shutter positions were adjusted to enable the synthesis of the thin films with the target compositional spread. The depositions were done onto r-cut sapphire substrates (MIR Enterprises) of 35 mm x 35 mm at a substrate temperature of 850 °C. The area of the materials compositional library on the substrate

was 28 mm x 28 mm. The thin film samples were cooled to room temperature before removal from the vacuum system for characterisation and screening.

The compositions of the thin films were measured using a Tescan Vega 3 Scanning Electron Microscope (SEM) equipped with an Oxford Instruments X-Max EDS detector on the thin films deposited on sapphire substrate. Sample charging was prevented by using copper tape to provide electrical continuity form the thin film to the sample mount. The compositional data was acquired using either a 14 x 14 macro (over 26 mm^2) or a 30 x 30 macro (over 28 mm^2). The crystal structure of the thin films was measured using a Bruker D8 diffractometer equipped with a Hi-Star GADDS 2D detector and correlated against published crystal structures from the ICDD database. The diffraction data was collected using a 14x14 macro (over 26 mm^2). The angles used for XRD were 11°for the incident angle and 25° for the detector angle. At this incident angle, the beam shape is an ellipse with a length of 1.05 mm and a width of 0.2 mm. The diffractograms were acquired for 200 s for each measurement.

Post deposition annealing of the thin films was carried out using a Rapid Thermal Processor (model JetFirst150 from Jipelec) using a reducing atmosphere of 5 wt% H_2 in Ar.

The thickness of the thin film was measured using optical profilometry (Veeco WYKO NT-1100 optical profilometer with a vertical resolution of 0.3 nm). In order to measure it, an equivalent thin film sample was coated with a uniform layer of gold by DC sputtering and its thickness around the edges was manually measured. Because of the relatively tight compositional variation of the sample the thickness was found to be relatively constant across the thin film at 415 nm.

The fluorescence of the thin films was measured using a purpose built screening apparatus, and this combined with the associated informatics platform enabled the rapid parallel measurement of the colour co-ordinate and relative quantum efficiency of fluorescence under blue LED excitation as a function of temperature. The screening apparatus comprises a light tight enclosure with matt black (anodised aluminium) internal surfaces to minimise reflection of light. Within the enclosure the thin film materials library on the 35 mm^2 substrate is mounted in a copper block which can be heated from room temperature to 300 °C. The front surface of the materials library is illuminated by blue light at 450nm from an LED (Thor Laboratories M455L3 royal blue LED) combined with a 450 ± 10 nm band pass filter in order to provide a well characterised illumination profile. The emitted fluorescent radiation in the visible region is measured using a Lumenera Infinity2-1M black and white camera (1392 x 1040 pixels @ 12 bit) imaging the entire front face of the library (29 mm^2 imaged over 800 x 800 pixels). The reflected illumination is removed using a 490 nm edge-pass filter (Edmund Optics) in front of the camera. Four images were recorded (typically averaged over 300 s) of the library, and four images of a blank substrate, with no additional filter, a blue SFK filter, a green SFK filter, and a red SFK filter (Schott Glass filter types SFK 100A, 101B and 102A from Skan House). An equivalent image of a blank substrate was subtracted from the sample images in order to eliminate any reflected background light, improving the reproducibility of the measurement. In order to convert the images from the camera to CIE 1931 values the spectral response of the individual filters and the camera where compared to the defined XYZ responses. A fitting routine was conducted using Matlab® to convert the combined response of the camera and filters to the required response producing simple factors to multiply the images by. The image data from each of the three filtered images was multiplied

by these factors to convert the image data into CIE 1931 XYZ values. The XYZ values were then normalised to provide Xbar and Ybar values. The validity of the measurements was assessed using three reference phosphors of known CIE1931 coordinates under 450 nm excitation and iteratively improving the factors until calibration from any two powders could be used to measure the third. The relative efficiency of the fluorescence of the materials was assessed using the image taken without the presence of the SFK filters. The intensity of this image was compared to the intensity of an image of a white alumina substrate taken without the presence of the edge pass filter in front of the camera, this allows the relative level of fluorescence to be compared across and between samples but does not provide quantum efficiency measurements. The sensitivity of the measurement allowed the averaging of the collected images in 25 x 25 pixel bins providing a 30 x 30 array of different materials in the library. These were then combined with the compositional and structural data of the materials library to provide a fast high-throughput measurement of the structural and compositional dependence of Xbar, Ybar and relative intensities of fluorescent light in the range 490 nm to ca. 700 nm). Thermal quenching of the fluorescent intensity was determined by carrying out the above series of imaging measurements at 25, 40, 50, 60, 70, 80, 90, 100, 110, 120 and 130°C and the CIE 1931 colour coordinates and relative efficiency extracted for the material at each of the temperatures.

Results and Discussion

In the following discussion the compositions of the films are referred with respect to the targeted and majority phase of $Ba_xSr_{2-x}SiO_4$ even in the case of regions with co-existence of several phases (as shown by XRD, see Figure 1 in supplementary

information). Therefore the x values represent the estimated values for a phase pure thin film.

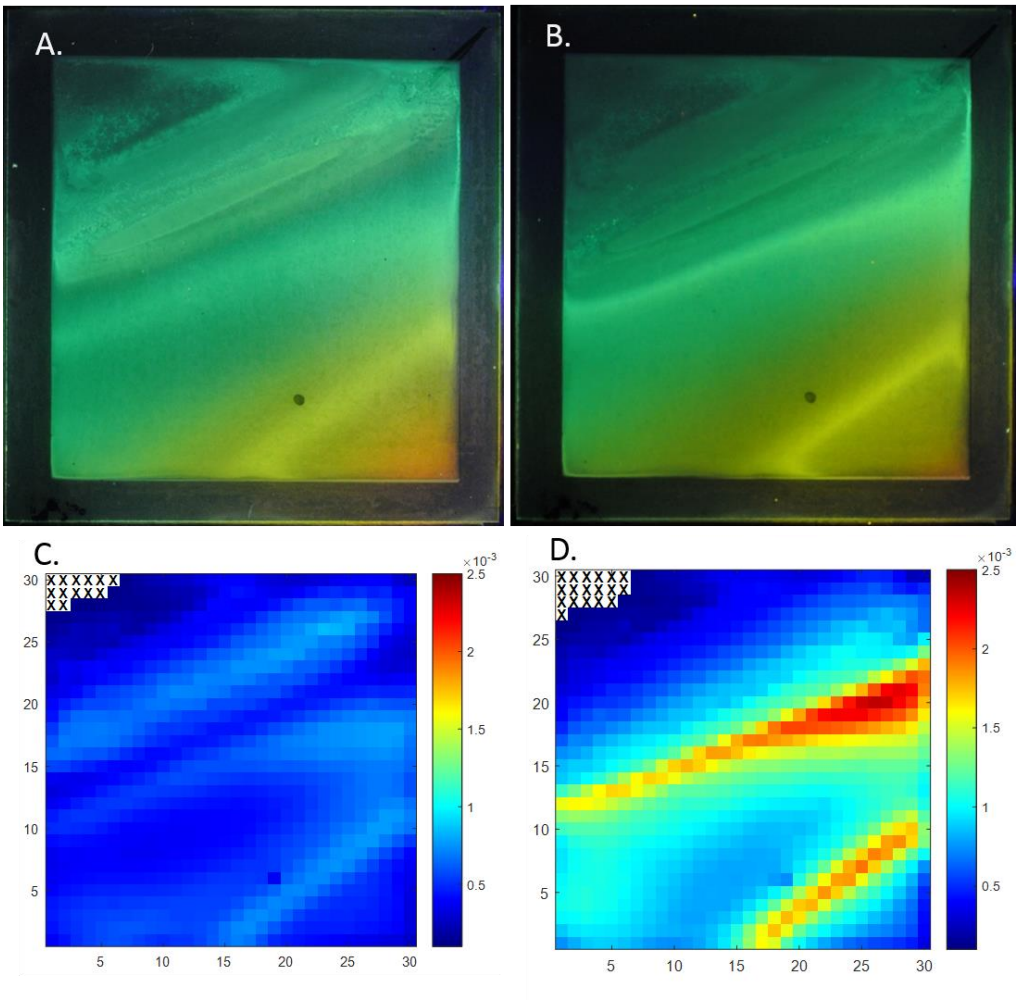

Figure 1: Images of the fluorescence observed on a $Sr_xBa_{2-x}SiO_4$ thin film library excited by 450 nm illumination. Images were obtained with a Nikon 1 J1 colour camera with an edge pass filter at 490 nm. The images correspond to the library (A) following reductive annealing for 30 mins at 600 °C (camera exposure time 15 s, F-stop: f/9) and (B) following reductive annealing for 30 mins at 700 °C (camera exposure time 3 s, F-stop: f/6.3). Plots (C) and (D) correspond to the relative efficiency of fluorescence measured using a black and white camera following the procedure detailed in the text. The relative efficiency scale is in arbitrary units, but the same relative scale is used in (C) and (D). A 30x30 matrix is used in the averaging of the fluorescent intensity across the sample.

Figure 1A and 1B show images of the direct observation of fluorescence from a Eu doped $Ba_xSr_{2-x}SiO_4$ thin film library using a colour digital camera (Nikon model 1-J1) and an edge pass filter at 490 nm in order to remove any reflected blue light from the excitation LED (450 nm). The image in Figure 1A was taken with an exposure time of 15 s (F-stop: f/9), and is the material library after annealing to 600 °C in a reducing atmosphere of 5% H_2 in Ar for 1800 s. The image shown in Figure 1B was taken with an exposure time of 3 s (F-stop: f/6.3) following the annealing of the material library at 700 °C under the same conditions. The shorter exposure time required to obtain the image reflects qualitatively the concomitant increase in fluorescent intensity induced by annealing at a higher temperature. This increase is also shown in Figures 1C and 1D which map the relative efficiencies across the thin film samples, measured using the black and white camera following the procedure detailed above, following annealing to, respectively, 600 °C and 700 °C. The colours displayed in the photographs vary diagonally in the images from orange to green, and this change can be attributed to relative concentrations of Ba and Sr substitution within the orthosilicate structure which is varying across the same diagonal. The target compositional spread of interest for the Eu doped $Ba_xSr_{2-x}SiO_4$ represents a Ba / Sr substitution with a constant amount of Si and Eu. The ideal concentration of Si is 33.33 at% and that of Eu is 2 at%. The deposition conditions for the thin film were adjusted to achieve opposite gradients of Ba and Sr and to keep the Si and Eu as constant as possible. The resulting compositional spread of the as-deposited thin film is shown in Figure 2. Large variations in the atomic percentages of both barium and strontium are observed as one element is substituted for the other. Smaller variations in both silicon (in the

range 30 - 34 at%) and europium (in the range 1.3 - 2.2 at%) are present and this

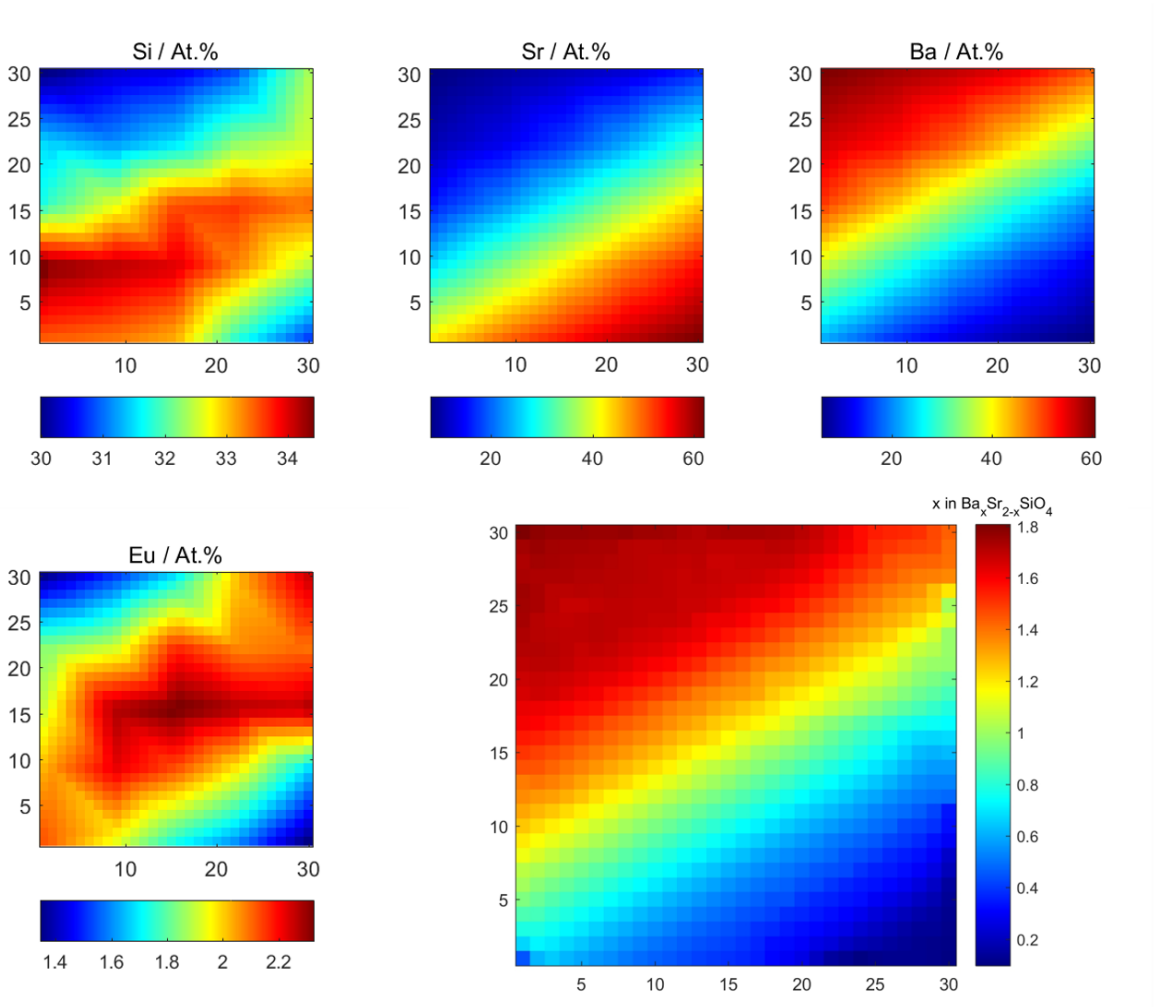

Figure 2: Elemental array maps of the constituent elements of Eu doped $Sr_xBa_{2-x}SiO_4$ (excluding oxygen) showing the variations as a function of position on the array. As well as map of x level in $Ba_xSr_{2-x}SiO_4$. Maps obtained by EDS using a 14x14 macro interpolated to 30x30.

small variation results in the synthesis because of the variation of the sum of barium and strontium as function of position on the array. Note that the thickness of the $Ba_xSr_{2-x}SiO_4$ library was relatively constant at 415 ± 54 nm. The compositional spread of the library shown in Figure 2 mapped onto the ternary space of Ba, Sr and Si is shown in Figure 3. The colour scale shows the compositional range of europium. The “as

synthesised" sample covers a narrow range of Si compositions (corresponding to the correct Si stoichiometry) and a broad range of Ba and Sr compositions. The europium concentration is in the range 1.3 – 2.2 at% as expected (Figure 2). Post reductive annealing at 600°C does not result in compositional or structural (see below) changes,

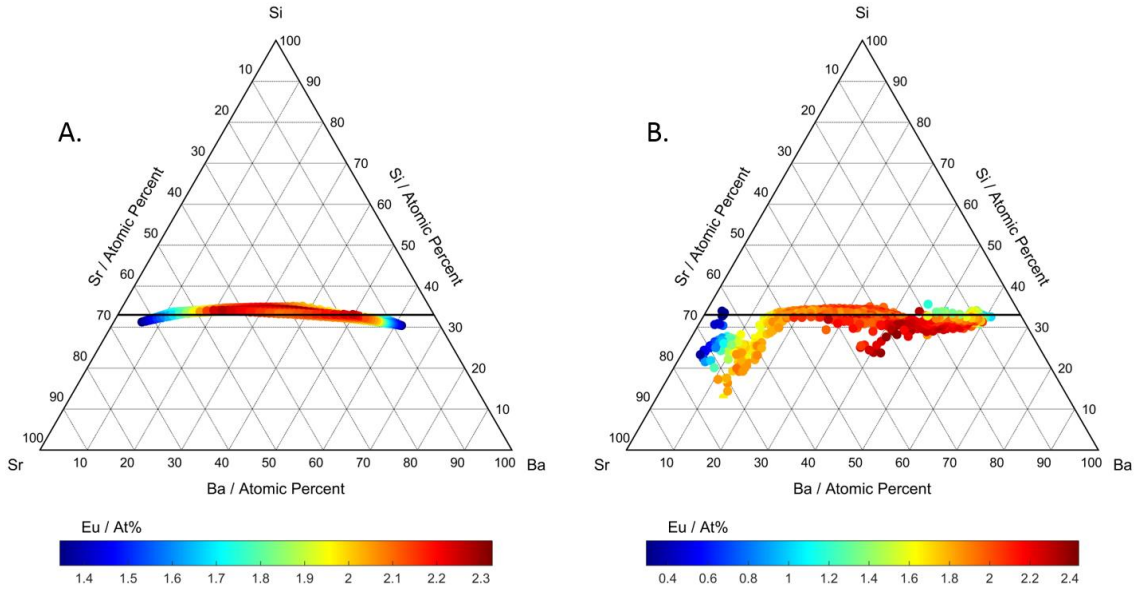

Figure 3: Ternary phase diagrams of the Eu doped $Ba_xSr_{2-x}SiO_4$ sample following deposition at 850 °C (A) and after annealing to 700 °C in 5% H_2 in Ar (B). The colour scale used represents the atomic percentage of europium. The tie-line at 33 at% Si represents the target composition of the orthosilicate structure (omitting the Eu).

but reductive annealing at 700°C results in apparent compositional changes for strontium rich compositions of the library (Figure 3B). This change corresponds to the apparent loss of ca. 15% Si for Sr compositions >85 at% with respect to Ba, although this corresponds to regions where the $Ba_xSr_{2-x}SiO_4$ is observed as phase pure (Figure 6C). We tentatively associate the apparent loss of Si with the reaction of the strontium rich $Ba_xSr_{2-x}SiO_4$ phase with the sapphire substrate (alumina) in reducing conditions at 700°C to produce aluminosilicate. The changes are limited to a region of the sample which changes from a two phases region to a single phase region, as determined by

XRD, upon annealing to 700 °C. Note that the europium concentration remains in the range 1.3 – 2.2 at% for most of the compositional range except for a small range of the very strontium rich compositions.

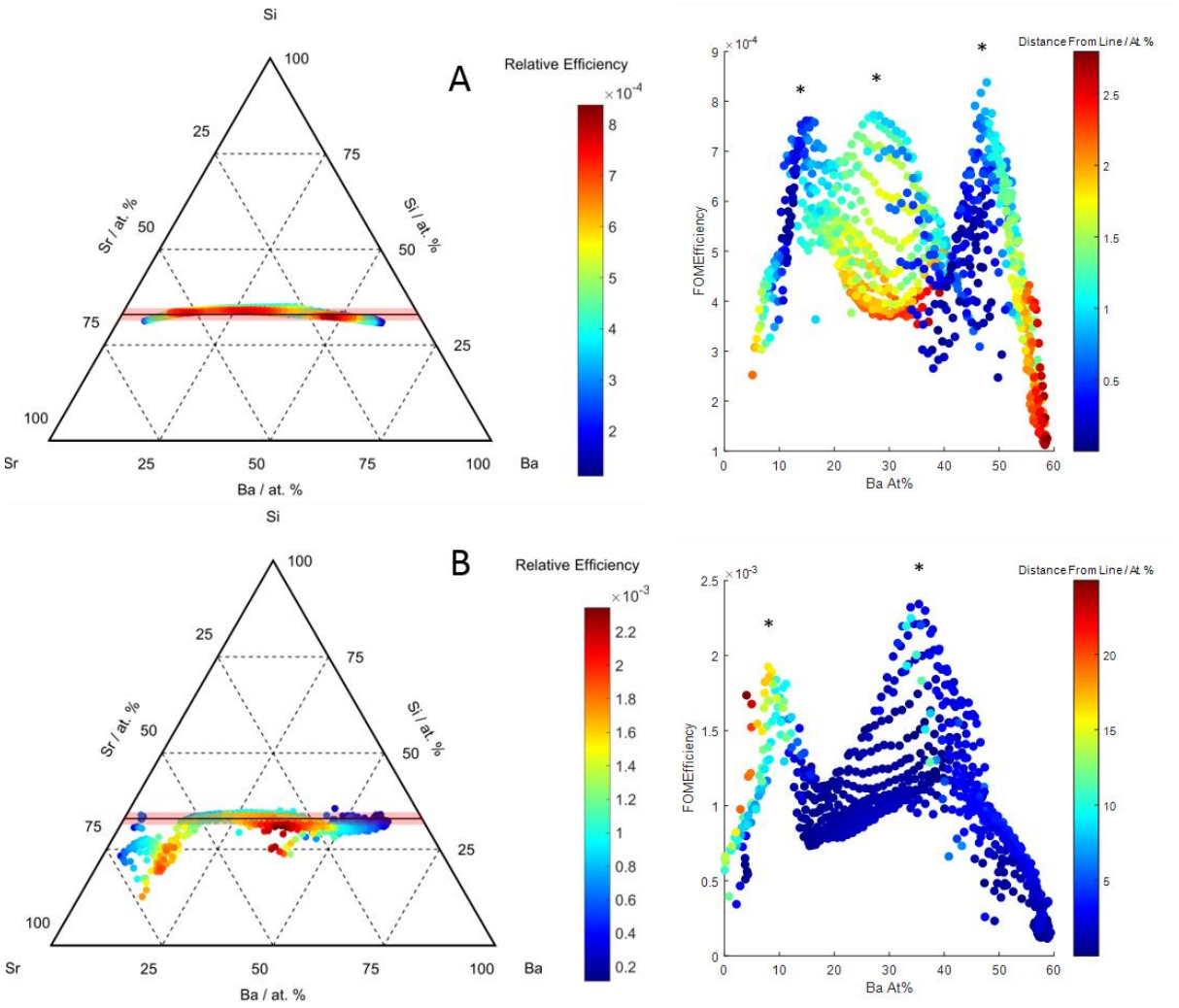

Figure 4: The relative quantum efficiencies of fluorescence for the $Ba_xSr_{2-x}SiO_4$ thin film library plotted in ternary compositional space, and as a function of Ba at% (averaged over Si compositions of +/- 2 at.%. Results are shown for the library following reductive annealing at A) 600◦C and B) 700◦C. The stars (*) represent the maxima used in Figure 5.

Figure 4 shows the relative quantum efficiency of the thin film phosphors following annealing at 600 °C and 700 °C in both ternary maps and as a function of the barium concentration. Similarly to what is shown in Figure 1 the relative quantum efficiency

increases significantly following annealing to the higher temperature. At both annealing temperatures, the observed maxima do not appear to be linked to any variation in europium concentration. Furthermore, the position of the maxima with respect to composition varies between the two annealing temperatures. The data obtained after annealing to 600 °C (Figure 4A) exhibits three maxima at 15, 27 and 48 at% barium where as after annealing to 700 °C two maxima are observed at 8 and 35 at% of barium. The position of these maxima with respect to the number of phases

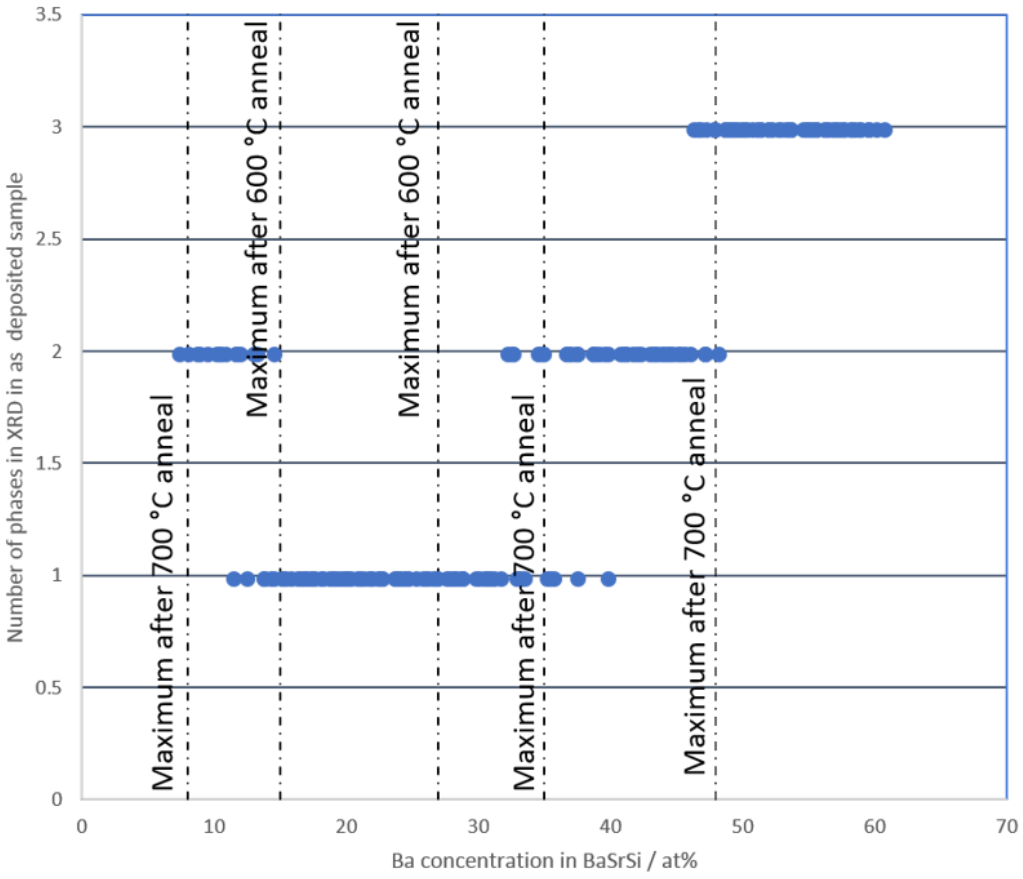

Figure 5: Number of phases measured by XRD in the as deposited sample as a function of the barium concentration. The vertical lines represent the position of the observed maxima in relative intensity after the two different annealing temperatures.

observed in the as deposited sample is shown in Figure 5. It can be seen that four of these maxima appear to be linked to the boundaries of the domain of existence of the

observed crystal phases and the changes occurring during the annealing. Only one (the one for 27 at% Ba form the 600 °C anneal) does not seem linked to any crystallographic change or boundary. It is therefore likely that the relative quantum efficiencies observed in our thin films are influenced both by optimal composition and grain sizes as well as the morphological changes induced by annealing. The loss of silicon observed for the strontium rich compositions might have caused a roughening of the material which in turn favours the emission and propagation of light.

The synthesis of the thin film $Ba_xSr_{2-x}SiO_4$ library was carried out on a substrate at 850°C to directly obtain a crystalline material during the synthesis. The target crystal structure was the barium / strontium orthosilicate structure (space group 62, *Pnma* or *Pmnb*). In order to achieve this, the elements were evaporated onto the substrate under a constant impinging flux of atomic oxygen. Typical diffractograms of four compositions of the "as deposited" sample are shown in Supplementary Material 1A. For all but the Ba rich compositions (Ba/Sr > ca. 3) the $Ba_xSr_{2-x}SiO_4$ orthorhombic (Space Group 62, *Pmnb*) structure dominates, except for a very small concentration of a minority Sr_3SiO_5 tetragonal phase (Space group 130, *P4/ncc*) at the highest Sr concentrations. The Ba rich compositions are characterised by a significant concentration of a secondary Ba_3SiO_5 tetragonal phase (Space group 130, *P4/ncc*). Even though the $Ba_xSr_{2-x}SiO_4$ orthorhombic is the predominant phase across the library, the fluorescence from this sample was very weak. Typical diffractograms of the library after reductive annealing to 600°C and 700°C are shown in Supplementary Material 1B and Supplementary Material 1C respectively. The Ba rich compositions have become predominantly the $Ba_xSr_{2-x}SiO_4$ orthorhombic phase at 600°C with a very low concentration of a minority phase identified as the $BaSiO_3$ rhombohedral phase (Space group 166, *R*-3*m*). The dominating peaks of the $Ba_xSr_{2-x}SiO_4$ phase show

some sharpening which is associated with developing crystallisation. Further reductive annealing of the library to 700°C results in further the sharpening of the peaks of the $Ba_xSr_{2-x}SiO_4$ phase associated with further crystal size growth, and a change of the minority phase from the $BaSiO_3$ rhombohedral phase to the $BaSiO_3$ orthorhombic phase in the Ba rich compositions. Note that the two regions of Sr and Ba rich compositions that exhibit the minority phases correspond to compositions of the as deposited library where the Si concentration is a few percent sub-stoichiometric relative to $Ba_xSr_{2-x}SiO_4$. This is evident in Figure 6 which shows the regions of $Ba_xSr_{2-x}SiO_4$ compositions which exhibit pure phases, and those compositions which also contain minority phases, as determined by XRD. It also highlights the changes observed upon annealing with the changes to the mixed phase regions towards a larger domain of existence of the single phase region of $Ba_xSr_{2-x}SiO_4$.

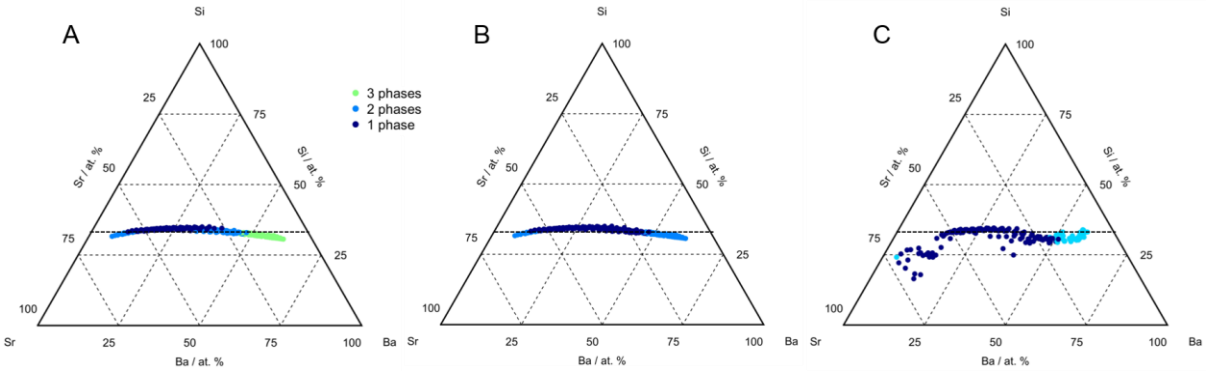

Figure 6: The number of additional phases identified in XRD (see Supplementary Information – Figure 2): Single phase $Ba_xSr_{2-x}SiO_4$ (dark blue), a single additional phase (light blue), two additional phases (green). These impurity phases were Sr_3SiO_5, Ba_3SiO_5 and $BaSiO_3$ and always seen at relatively low concentrations. Results are shown for A) the as deposited library, and following reductive annealing at at A) 600◦C and B) 700◦C.

The fluorescence of the thin film $Sr_xBa_{2-x}SiO_4$ material was measured on the as-deposited library (i.e. after synthesis at 850 °C), and after annealing to 600 °C and 700 °C. The library did not display significant fluorescence at any composition in the as-deposited state. The absence of fluorescence could be due to the absence of the $Ba_xSr_{2-x}SiO_4$ crystalline phases, or the incorrect oxidation state of the activator, i.e. Eu^{3+} rather than Eu^{2+}. Since the correct crystalline phase is already substantially formed in the as deposited samples (Figure 6A) we believe that it is the incorrect oxidation state of the europium that accounts primarily for the weak fluorescence, the oxidising conditions of the direct synthesis resulting in predominantly Eu^{3+}. Reduction of Eu^{3+} to Eu^{2+} was subsequently induced through the reductive annealing step. We were, unfortunately, unable to confirm this change in oxidation state by XPS through lack of sufficient signal to noise in the measurement of any of the Eu transitions.

The fluorescence of the $Ba_xSr_{2-x}SiO_4$ library, following reductive annealing at 600°C and 700°C, was measured at a substrate temperature of 25°C. Using the procedure described above with the black and white camera and filters, the sequence of images was processed to determine the relative quantum efficiency (Figure 1 and 4) and the CIE 1931 colour coordinates of the fluorescent radiation. The relative quantum efficiency and the solid solution concentration x in $Ba_xSr_{2-x}SiO_4$ is plotted as a function of CIE co-ordinates in Figure 7. The 30 x 30 grid of the image results in a variation of composition for each point in the library of ≤ 1 at%. The relative quantum yield across the sample assessed with the black and white camera (Figure 1C and 1D) reassuringly closely mimics the trend observed in fluorescent intensity measured with the colour camera (Figure 1A and 1B). The units of the relative quantum yield are arbitrary, but

the same used in the case of the samples reductively annealed at the two

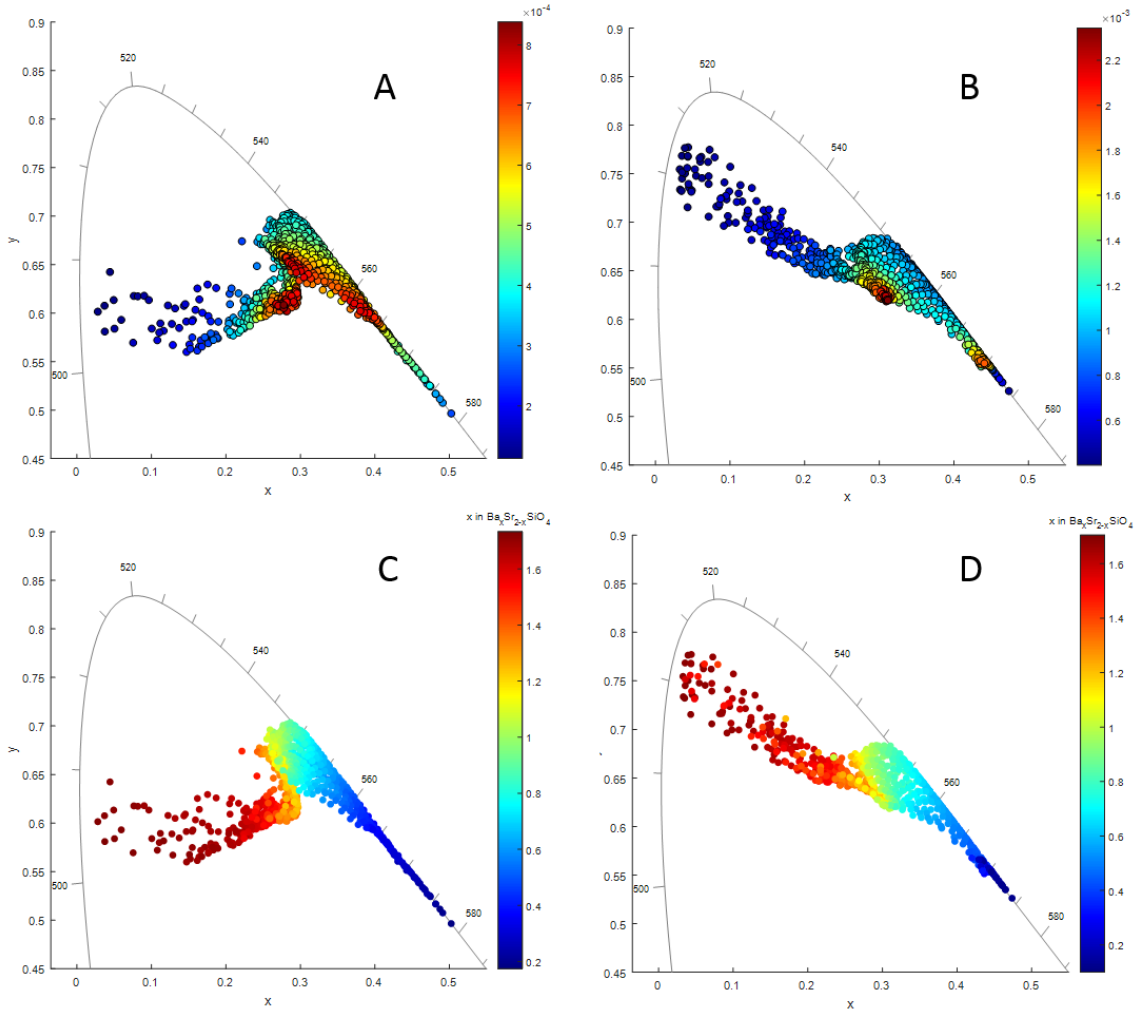

Figure 7: CIE plots of fluorescence observed on thin film samples of Eu doped $Ba_xSr_{2-x}SiO_4$ synthesised at 850 °C and annealed at 600 °C (A. and C.) and 700 °C (B. and D.) in 5% H_2 in Ar. A. and B. display the relative quantum efficiencies as a function of CIE values and C. and D. use the x in $Ba_{2-x}Sr_xSiO_4$ as coloured figure of merit.

temperatures: The intensity of fluorescence (Figure 1 and 4) is increased for the majority of compositions by annealing at the higher temperature, with the Ba rich phases exhibiting the smallest change. This may be associated with the increase in crystallite size evident in the diffraction (Supplementary Information – Figure 1) or a further reduction in the Eu to Eu^{2+}. The strong modulation of the relative quantum yield in the library annealed at 700°C (Figure 1C and Figure 4B) is not correlated with the

small changes in Eu concentration in the sample (Figure 2) and is rather associated with the $Ba_xSr_{2-x}SiO_4$ orthorhombic phase itself. There also appears to be no simple $Ba_xSr_{2-x}SiO_4$ compositional dependence (Figure 4) associated with the relative quantum efficiency after reductive annealing at 600°C, although after reductive annealing at 700°C, the compositions exhibiting the lowest quantum yields correspond to regions of both high values of x in $Ba_xSr_{2-x}SiO_4$ which contain small concentration of secondary phases. Since the quantum yield appears very sensitive to the extent of crystallisation, evidenced by the order of magnitude changes associated with higher temperature annealing, it is also likely that the relative quantum yield across composition is also influenced by differences in the crystalline morphology in the thin film library.

The CIE 1931 colour coordinates of the fluorescent radiation for the library after reductive annealing at 600°C and 700°C Figure 7A, 7C and Figure 7B, 7D respectively. The colour scale of the points represents the relative quantum yield in the case of Figure 7A and 7B, whereas Figure 7C and 7D plot the compositional dependence of the CIE coordinates. For the library annealed at 600°C, a significant proportion of the compositional library exhibit fluorescence with CIE 1931 colour coordinates on, or close to, the spectral locus corresponding to monochromatic emission between 580-545nm (the yellow/orange into the green region of pure hue). Figure 7C show that these compositions correspond to $1.15 > x > 0.17$ in $Ba_xSr_{2-x}SiO_4$: The yellow/orange region is associated with the strontium rich compositions, and the green region with the higher Ba compositions. A second group of points, corresponding to Ba rich compositions with $1.77 > x > 1.18$ (Figure 7C), can be identified which are in a region well away from the spectral locus corresponding to colours with multiple emission bands and low relative quantum yield.

The two groups of compositional points identified above behave differently on reductive annealing at 700°C (Figure 7C and Figure 7D). The component of the library with compositions 1.15 > x > 0.17 on or close to the spectral locus largely remain, although the region along the locus shrinks to between 575-550 nm. For the second group of Ba rich compositions with 1.77 > x > 1.18 these $Ba_xSr_{2-x}SiO_4$ compositions associated with the multiple colour bands become more green in their fluorescence with an increase in Ybar values.

In general these results are in agreement with similar studies in terms of compositional dependence of the fluorescence with the $Ba_xSr_{2-x}SiO_4$:Eu system.[26]

The line delimiting the two regions (barium rich and strontium rich, around x = 1.15) appears well defined on the thin sample and in the corresponding CIE 1931 colour space, it also follows the transition region between the pure orthosilicate and the mixed orthosilicate/Ba_3SiO_5. The fact that the demarcation line seen in the thin film sample corresponds to compositions with 1.1 < x < 1.3 in $Ba_xSr_{2-x}Si_{1.94}Eu_{0.06}O_4$ would indicate that the transition is less driven by composition but more by the phase purity of the as-deposited thin film. However, the $Ba_xSr_{2-x}Si_{1.94}Eu_{0.06}O_4$ formula is a target composition and the reality, as shown in Figure 2, is that the Si varies across the array between 30 and 34 at%. This variation influences the phase purity of the synthesised thin film, in our case we have seen that the phase pure orthosilicate exists for silicon between 32.5 and 34 at%.

Observation and analysis of the results indicate that the ideal annealing temperature for these materials is, either, composition dependent or phase purity dependant. Compositions with more than 56 at% Sr (excluding oxygen) or x < 0.33 in $Ba_xSr_{2-x}Si_{1.94}Eu_{0.06}O_4$ being adversely affected by annealing at 700 °C with a decrease in the

associated wavelength and a shift from orange to a more yellow colour. In the case of the barium rich region (x > 1.2) the changes caused by the annealing to 700 °C are pronounced in terms of colour characteristics CIE Xbar and Ybar, but not in terms of intensities. This correlation indicates a composition dependence of the required annealing temperature, however these limits in x also match quite closely the phase purity as seen by XRD. At this stage, it would be difficult to conclude either way, the studies of fluorescent thin films is limited and no technique similar to ours has ever been used to synthesise fluorescent thin films. The only comparison is with bulk powder synthesised by more classical reaction routes. For these the annealing temperatures reported are much higher and we are not aware of composition dependence of annealing temperatures within a family of compound.

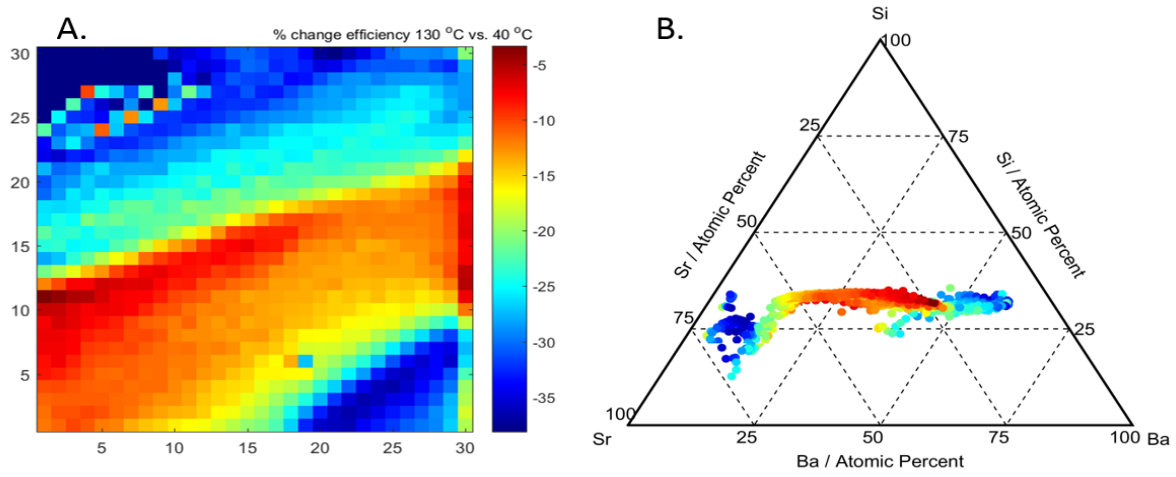

Figure 8: Thermal quenching. Percentage of change in relative quantum yield between the fluorescence measured at 130 °C vs 40°C, in array map (A) and in pseudo ternary plot (Eu omitted) (B). Sample annealed to 600 °C.

The thermal quenching of the fluorescence has been measured between 25-130°C. The effect of thermal quenching is important in the application of down-shifting phosphors in LED applications because of the range of temperatures during operation.

The fluorescence of the $Ba_xSr_{2-x}SiO_4$ library, following reductive annealing at 600°C, was measured at a number of substrate temperatures in the range 25-130°C. Using the procedure described above with the black and white camera and filters, the sequence of images was processed to determine the relative quantum yield and the CIE 1931 colour coordinates of the fluorescent radiation on a 30 x 30 grid. The effect of temperature on the CEI colour coordinates and quantum yield for six compositions of the library is shown in supplementary material – Figure 2. There are no significant changes in the CIE 1931 Xbar colour coordinate of the fluorescent radiation in the measured temperature range (supplementary material – Figure 2A) although some change in the Ybar colour coordinate (supplementary material – Figure 2B) is observed at temperatures above 100°C for a few of the compositions with the changes seemingly increasing with increasing Ba concentration. Larger changes are observed (reductions) in the relative quantum yields with increasing temperature (supplementary material – Figure 2C): The changes are greatest (accelerate) above 100°C for all compositions. In order to understand the compositional and phase dependence of this apparent thermal quenching of the $Ba_xSr_{2-x}SiO_4$ phosphors, the percentage reduction in quantum yield between 40°C and 130°C is plotted across the sample library (Figure 8A) and as a function of composition (Figure 8B). The sample library is characterised by a broad band of $Ba_xSr_{2-x}SiO_4$ compositions which undergo the least thermal quenching (<20%), and these correspond to compositions with $1.36 > x > 0.39$. Compositions which are Ba or Sr rich outside of this range exhibit a higher degree of thermal quenching. The limits of the band of stable phosphors matches very well the two bands of highest relative quantum yield shown in Figure 1D. This delimits some relatively important stoichiometry with the silicon concentration in excess of 32 at% (see Figure 2) but also delimits the transition between the region of pure

orthosilicate from the as deposited phase and the regions of mixed phases. The higher relative quantum yield observed for these regions, when compared to the yield in the centre of the band of pure orthosilicate, would suggest that the increase in phase purity seen in these regions during the annealing is responsible for the increase in relative quantum yield.

Conclusions

We have shown the first use of reactive thermal evaporation using HT-PVD for the synthesis of thin films of europium doped barium strontium orthosilicates on sapphire substrates. The thin films synthesised at 850 °C show the existence of a predominant orthosilicate phase throughout the range of compositions investigated. This phase has been found, by XRD, to be pure in the as deposited state for $0.39 < x < 1.07$ in $Ba_xSr_{2-x}Si_{1.96}Eu_{0.04}O_4$, this domain of pure phase increases to $0.39 < x < 1.39$ following annealing to 600°C in reducing atmosphere. A primary parallel screen and associated informatics tools has been developed which enables the rapid assessment of the fluorescence of the thin films. Using these tools, we have reported the first direct observation of fluorescence in a thin film produced by reactive evaporation. The fluorescence has been mapped using CIE 1931 coordinates. A trend in colour variation from yellow to yellow green as the ratio of strontium to barium decreases has been observed. This trend matches well that of commercial powders proving that combinatorial thin film synthesis and high throughput techniques can be used to study phosphor materials and assess the effects of composition variations and phase purity on the material properties. Our fluorescence primary screen enables rapid characterisation of relative intensities and colour coordinates as well as allowing the thermal stability of the material to be measured. The relative quantum yield shows

maximums linked to both compositional variations and a purification process during annealing at the boundaries between regions of pure orthosilicate and mixed phases. The thermal stability study of the thin films shows that regions of pure orthosilicate from the as-deposited state exhibit losses of < 20% when operating at 130 °C.

Application of this approach to other systems can easily be done, these could be studies of orthosilicate crystal structure with different active elements, or different alkaline cations, or a different crystal structure as host to the active element.

Supporting information

Selected diffractograms of Eu doped $Ba_xSr_{2-x}SiO_4$ for selected compositions, diffractograms shown for the as deposited thin film and after annealing to 600 °C and 700 °C.

Thermal quenching experiment for selected compositions showing variations in CIE X, CIE Y and relative quantum efficiency as a function of temperature.

References

1. Barry, T. L. Fluorescence of Eu^{2+} activated phases in binary alkaline earth orthosilicate systems. *J. Electrochem. Soc* **1968,** *115* (11), 1183.

2. Blasse, G.; Bril, A. Photoluminescent efficiency of phosphors with electronic transitions in localized centers. *J. Electrochem. Soc* **1968,** *115* (10), 1067.

3. Bril, A.; Blasse, G.; Bertens, J. A. A. Measurement of quantum efficiencies of Eu^{3+} activated phosphors using excitation to selected Eu^{3+} levels. *J. Electrochem. Soc* **1968,** *115* (4), 395.

4. Wang, J. S.; Yoo, Y.; Gao, C.; Takeuchi, I.; Sun, X. D.; Chang, H. Y.; Xiang, X. D.; Schultz, P. G. Identification of a blue photoluminescent composite material from a combinatorial library. *Science* **1998,** *279* (5357), 1712-1714.

5. Braun, C.; Seibald, M.; Boerger, S. L.; Oeckler, O.; Boyko, T. D.; Moewes, A.; Miehe, G.; Tuecks, A.; Schnick, W. Material properties and structural characterization of $M_3Si_6O_{12}N_2$:Eu^{2+} (M = Ba, Sr)-A comprehensive study on a promising green phosphor for pc-LEDs. *Chem. - Eur. J.* **2010,** *16* (31), 9646-9657.

6. Brgoch, J.; Kloss, S. D.; Denault, K. A.; Seshadri, R. Accessing ($Ba_{1-x}Sr_x$) $Al_2Si_2O_8$: Eu phosphors for solid state white lighting via microwave- assisted preparation: tuning emission color by coordination environment. *Z. Anorg. Allg. Chem* **2014,** *640* (6), 1182-1189.

7. Hua, Y.; Ma, H.; Deng, D.; Zhao, S.; Huang, L.; Wang, H.; Xu, S. Enhanced photoluminescence properties of orange emitting $Sr_{2.96-x}Ba_xSiO_5$: Eu^{2+} phosphors synthesized with Sr_2SiO_4 as precursor. *J. Lumin.* **2014,** *148*, 39-43.

8. Park, J. K.; Lim, M. A.; Kim, C. H.; Park, H. D.; Park, J. T.; Choi, S. Y. White light-emitting diodes of GaN-based Sr_2SiO_4 : Eu and the luminescent properties. *Applied Physics Letters* **2003,** *82* (5), 683-685.

9. Yang, C.-C.; Lin, C.-M.; Chen, Y.-J.; Wu, Y.-T.; Chuang, S.-R.; Liu, R.-S.; Hu, S.-F. Highly stable three-band white light from an InGaN-based blue light-emitting diode chip precoated with (oxy)nitride green/red phosphors. *Appl. Phys. Lett.* **2007,** *90* (12) 123503.

10. Zeuner, M.; Pagano, S.; Schnick, W. Nitridosilicates and oxonitridosilicates: from ceramic materials to structural and functional diversity. *Angew. Chem. Int. Ed* **2011,** *50* (34), 7754-7775.

11. Chen, L.; Chen, K.-J.; Hu, S.-F.; Liu, S. Combinatorial chemistry approach to searching phosphors for white light-emitting diodes in (Gd-Y-Bi-Eu)VO_4 quaternary system. *J. Mater. Chem.* **2011,** *21* (11), 3677-3685.

12. Jung, Y. S.; Kulshreshtha, C.; Kim, J. S.; Shin, N.; Sohn, K.-S. Genetic algorithm-assisted conbinatorial search for new blue phosphors in a$(Ca,Sr,Ba,Mg,Eu)_{(x)}B_yP_zO$ delta system. *Chem. Mater.* **2007,** *19* (22), 5309-5318.

13. Park, J. K.; Choi, K. J.; Kim, K. N.; Kim, C. H. Investigation of strontium silicate yellow phosphors for white light emitting diodes from a combinatorial chemistry. *Appl. Phys. Lett.* **2005,** *87* (3) 031108.

14. Park, J. K.; Lim, M. A.; Choi, K. J.; Kim, C. H. Luminescence characteristics of yellow emitting $Ba_3SiO_5 : Eu^{2+}$ phosphor. *J. Mater. Sci.* **2005,** *40* (8), 2069-2071.

15. Zhou, L.; Jiao, H.; He, D. Search for new phosphors in Eu^{2+} doped $MgAl_2O_4$-$SrAl_2O_4$-$BaAl_2O_4$ ternary system by combinatorial approach. *Mater. Chem. Phys.* **2011,** *127* (1-2), 227-231.

16. Lee, B.; Lee, S.; Jeong, H. G.; Sohn, K.-S. Solid-state combinatorial screening of $(Sr,Ca,Ba,Mg)_{(2)}Si_5N_8:Eu^{2+}$ phosphors. *ACS Comb. Sci.* **2011,** *13* (2), 154-158.

17. Park, W. B.; Shin, N.; Hong, K.-P.; Pyo, M.; Sohn, K.-S. A new paradigm for materials discovery: heuristics-assisted combinatorial chemistry involving parameterization of material novelty. *Adv. Funct. Mater.* **2012,** *22* (11), 2258-2266.

18. Park, W. B.; Singh, S. P.; Yoon, C.; Sohn, K.-S. Combinatorial chemistry of oxynitride phosphors and discovery of a novel phosphor for use in light emitting diodes, $Ca_{1.5}Ba_{0.5}Si_5N_6O_3:Eu^{2+}$. *J. Mater. Chem. C* **2013,** *1* (9), 1832-1839.

19. Mordkovich, V. Z.; Jin, Z. W.; Yamada, Y.; Fukumura, T.; Kawasaki, M.; Koinuma, H. Fabrication and characterization of thin-film phosphor combinatorial libraries. *Solid State Sci.* **2002,** *4* (6), 779-782.

20. Danielson, E.; Devenney, M.; Giaquinta, D. M.; Golden, J. H.; Haushalter, R. C.; McFarland, E. W.; Poojary, D. M.; Reaves, C. M.; Weinberg, W. H.; Wu, X. D. A rare-earth phosphor containing one-dimensional chains identified through combinatorial methods. *Science* **1998,** *279* (5352), 837-839.

21. Danielson, E.; Golden, J. H.; McFarland, E. W.; Reaves, C. M.; Weinberg, W. H.; Wu, X. D. A combinatorial approach to the discovery and optimization of luminescent materials. *Nature* **1997,** *389* (6654), 944-948.

22. Guerin, S.; Hayden, B. E. Physical vapor deposition method for the high-throughput synthesis of solid-state material libraries. *J. Comb. Chem.,* **2006,** *8* (1), 66-73.

23. George, N. C.; Denault, K. A.; Seshadri, R. Phosphors for Solid-State White Lighting. *Annu. Rev. Mater. Res., Vol 43*, Clarke, D. R., Ed. 2013; Vol. 43, pp 481-501.

24. Lim, M. A.; Park, J. K.; Kim, C. H.; Park, H. D.; Han, M. W. Luminescence characteristics of green light emitting Ba_2SiO_4 : Eu^{2+} phosphor. *J. Mater. Sci. Lett.* **2003,** *22* (19), 1351-1353.

25. Chen, Y. C.; Nien, Y. T. Microstructure and photoluminescence properties of laser sintered YAG:Ce phosphor ceramics. *J. Eur. Ceram. Soc.* **2017,** *37* (1), 223-227.

26. Denault, K. A.; Brgoch, J.; Gaultois, M. W.; Mikhailovsky, A.; Petry, R.; Winkler, H.; DenBaars, S. P.; Seshadri, R. Consequences of optimal bond valence on structural rigidity and improved luminescence properties in $Sr_xBa_{2-x}SiO_4$:Eu^{2+} orthosilicate phosphors. *Chem. Mater.* **2014,** *26* (7), 2275-2282.

27. Heindl, R.; Amara, A.; Tary, G.; Loriers, J.; Lignou, F. On the polymorphism of Sr_2SiO_4 - A high-pressure monoclinic phase and an orthorhombic phase. *J. Mater. Sci. Lett.* **1985,** *4* (12), 1449-1450.

28. Lee, J. S.; Kim, Y. J. Effects of barium on luminescent properties of $Sr_{2-x}Ba_xSiO_4$:Eu^{2+} nanoparticles. *Ceram. Int.* **2013,** *39*, S555-S558.

29. Yoo, J. S.; Kim, S. H.; Yoo, W. T.; Hong, G. Y.; Kim, K. P.; Rowland, J.; Holloway, P. H. Control of spectral properties of strontium-alkaline earth-silicate-europium phosphors for LED applications. *J. Electrochem. Soc.* **2005,** *152* (5), G382-G385.

30. He, L. H.; Zou, X.; Wang, T.; Zheng, Q. J.; Jiang, N.; Xu, C. G.; Liu, Y. F.; Lin, D. M. Red/blue-shift dual-directional regulation in blue-emitting $Ca_{0.8}Ba_{1.2}SiO_4:Eu^{2+}$ phosphor on incorporation of Eu^{2+}/Mg^{2+} ions. *J. Electron. Mater.* **2017,** *46* (3), 1777-1786.

31. Lin, Y. T.; Niu, Z. R.; Han, Y.; Li, C. Z.; Zhou, W. L.; Zhang, J. L.; Yu, L. P.; Lian, S. X. The self-reduction ability of RE^{3+} in orthosilicate (RE = Eu, Tm, Yb, Sm): $BaZnSiO_4$-based phosphors prepared in air and its luminescence. *J. Alloys Compd.* **2017,** *690*, 267-273.

32. Ozturk, E.; Karacaoglu, E. Dy^{3+}-activated M2SiO4 (M = Ba, Mg, Sr)-type phosphors. *Bull. Mater. Sci.* **2017,** *40* (1), 25-30.

33. Xue, N.; Hei, Z. F.; Zhao, Z.; Wang, J.; Wang, T.; Li, M. X.; Noh, H. M.; Jeong, J. H.; Yu, R. J. Preparation and luminescent properties of Sm^{3+}-doped high thermal stable sodium yttrium orthosilicate phosphor. *J. Nanosci. Nanotechnol.* **2016,** *16* (4), 3500-3505.

34. Zhang, J. L.; Zhang, W. L.; Qiu, Z. X.; Zhou, W. L.; Yu, L. P.; Li, Z. Q.; Lian, S. X. $Li_4SrCa(SiO_4)(2):Ce^{3+}$, a highly efficient near-UV and blue emitting orthosilicate phosphor. *J. Alloys Compd.* **2015,** *646*, 315-320.

35. Wang, Q.; Qiu, J.-B.; Song, Z.-G.; Zhou, D.-C.; Xu, X.-H. Green long-after-glow luminescence of Tb^{3+} in Sr_2SiO_4. *Chin. Phys. B* **2014,** *23* (6) 064211.

36. Baginskiy, I.; Liu, R. S.; Wang, C. L.; Lin, R. T.; Yao, Y. J. Temperature dependent emission of strontium-barium orthosilicate $(Sr_{2-x}Ba_x)SiO_4:Eu^{2+}$ phosphors for high-power white light-emitting diodes. *J. Electrochem. Soc.* **2011,** *158* (10), P118-P121.